Lab on a Chip

Digital quantification and selection of high-lipid-producing microalgae through a lateral dielectrophoresis-based microfluidic platform

Journal:	*Lab on a Chip*
Manuscript ID	LC-ART-08-2019-000850.R1
Article Type:	Paper
Date Submitted by the Author:	30-Oct-2019
Complete List of Authors:	Han, Song-I; Texas A&M University College Station, Kim, Hyun Soo; Korea Institute of Machinery and Materials, Daegu Research Center for Medical Devices and Rehabilitation Han, Ki-Ho; Inje University - Gimhae Campus, Department of Nanoscience and Engineering Han, Arum; Texas A&M University College Station

PAPER

Received 00th January 20xx,
Accepted 00th January 20xx
DOI: 10.1039/x0xx00000x

Digital quantification and selection of high-lipid-producing microalgae through a lateral dielectrophoresis-based microfluidic platform

Song-I Han‡[a], Hyun Soo Kim‡[b], Ki-Ho Han[c] and Arum Han*[a,d]

Microalgae are promising alternatives to petroleum as renewable biofuel sources, however not sufficiently economically competitive yet. Here, a label-free lateral dielectrophoresis-based microfluidic sorting platform that can digitally quantifiy and separate microalgae into six outlets based on the degree of their intracellular lipid content is presented. In this microfluidic system, the degree of cellular lateral displacement is inversely proportional to the intracellular lipid level, which was successfully demonstrated using *Chlamydomonas reinhardtii* cells. Using this functionality, a quick digital quantification of sub-populations that contain different intracellular lipid level in a given population was achieved. In addition, the degree of lateral displacement of microalgae could be readily controlled by simply changing the applied DEP voltage, where the level of gating in the intracellular lipid-based sorting decision could be easily adjusted. This allowed for selecting only a very small percentage of a given population that showed the highest degree of intracellular lipid content. In addition, this approach was utilized through an iterative selection process on natural and chemically mutated microalgal populations, successfully resulting in enrichment of high-lipid-accumulating microalgae. In summary, the developed platform can be exploited to quickly quantify microalgae lipid distribution in a given population in real-time and label-free, as well as to enrich a cell population with high-lipid-producing cells, or to select high-lipid-accumulating microalgal variants from a microalgal library.

1. Introduction

Microalgae, photosynthetic microorganisms that convert sunlight, water, and CO2 into biomass and lipids, have been widely cultivated to produce various high-value products such as pharmaceuticals, cosmetics, pigments, animal feed, bioplastics, and functional foods [1-3]. Moreover, microalgae have been highlighted as promising resources for renewable biofuel due to increasing concerns over limited fossil fuel reserves as well as CO2 emission [4-6]. Compared to other biofuel feedstock (e.g., oil crops), microalgae hold several advantages such as higher photosynthetic efficiency, faster growth rate, higher lipid productivity, higher CO_2 fixation capacity, and less competition with food sources and land usage [7]. Despite these promising potentials, the production cost of microalgae-based biofuels is still not economically competitive, and thus, significant improvements are necessary throughout the entire algal biofuel development pipeline, including strain selection and development, cultivation, harvesting, lipid extraction, and conversion [8, 9].

Monitoring and quantification of intracellular lipid level during microalgal cultivation, which can provide essential information to achieve precise process control and productivity improvement, have been achieved based on fluorometry, infrared (IR) radiation including mid-IR, near-IR, and Fourier transform IR, and flow cytometry [10]. Even though high-throughput and label-free quantification of lipid level can be achieved by these systems, these methods typically require additional sample preparation steps or complicated instrumentations. These challenges have so far limited the wide-spread use of these technology development to be exploited for real-time onsite monitoring and quantification of lipid level of microalgae.

Selection of microalgal strains with high lipid level through screening from natural habitats or from microalgal libraries generated through metabolic engineering and/or mutagenesis is one of the promising strategies to develop and obtain strains with higher lipid productivity [11, 12]. This strain selection process typically requires single-cell resolution analysis of lipid content from a large number of sample populations, since each microalgal cell in a given library is a potential variant that has different attributes. However, conventional screening and selection methods utilizing dilution-based multi-well plate culture are labor-intensive and time-consuming, and thus limited in throughput as well as the library size that can be screened [13, 14]. Other methods such as fluorescence-activated cell sorting (FACS) and imaging flow cytometry have been successfully used to screen and select high-lipid-producing mutants [15-17], as these instruments can provide orders of magnitude higher throughput compared to conventional well-plate assays. However, in all of these methods, cells have to be first fluorescently stained for examining their intracellular lipid content, thus adding additional assay steps, time, and cost is needed.

Recently, several microfluidic approaches have been developed and applied to speed up the microalgal strain development processes, cultivation condition testing steps [18-22], and label-free lipid

a. Department of Electrical and Computer Engineering, Texas A&M University, College Station, TX 77843, USA
b. Korea Institute of Machinery and Materials, Daegu Research Center for Medical Devices and Rehabilitation, Daegu, 42994, Republic of Korea
c. Department of Nanoscience and Engineering, Center for Nano Manufacturing, Inje University, Gimhae, 50834, Republic of Korea
d. Department of Biomedical Engineering, Texas A&M University, College Station, TX 77843, USA
†Electronic Supplementary Information (ESI) available: See DOI: 10.1039/x0xx00000x
‡These authors contributed equally to this work.

quantification [23]. As an example of microfluidic systems as strain development tools, a simple microfluidic device that can separate cells having faster phototactic response was successfully utilized to find mutants having faster growth rate and higher lipid level [20, 24]. In another example, a high-throughput droplet microfluidics-based screening platform has been developed and successfully utilized to screen and isolate fast-growing and/or high-lipid-producing mutants [25-27]. In that droplet microfluidics platform, large numbers of cell-encapsulated water-in-oil emulsion droplets were utilized, each droplet functioning as individual pico-liter-scale bioreactors, for analyzing the cellular attributes (e.g., growth rate and lipid content) of each microalgal variant encapsulated within. Although these microfluidics-based technologies are extremely efficient and powerful for selecting microalgal strains with higher lipid content, they still require an intracellular lipid staining step that can either negatively affect the cells or add additional processing steps, as well as somewhat difficult to utilize without expertise in microfluidics. An ideal system should be able to rapidly screen, select, and sort individual cells based on their intracellular lipid quantity in a label-free manner.

Dielectrophoresis (DEP) is a label-free, real-time, and electric field-based cell manipulation technique, which can be readily realized in a microfluidic format, since only a simple microfluidic channel integrated with electrodes is required. Thus, DEP-based cell manipulation methods have been extensively utilized in various cell manipulation applications [28, 29]. When cells pass through an electrode pair where a non-uniform alternating current (AC) electric field is generated, cells either experience a positive DEP (pDEP) force (i.e., towards the electrodes) or a negative DEP (nDEP) force (i.e., away from the electrodes). The polarity and magnitude of DEP force are determined by the dielectric properties of cells and surrounding solution, the size of cell, as well as the applied voltage and frequency. This difference in DEP force depending on cell properties can be utilized to change the trajectories of cells flowing inside a microfluidic channel, enabling cell manipulation and cell separation.

Although DEP has been demonstrated as an effective tool in cell separation, most applications have been focused on mammalian cells [30-32] and bacteria [33], and only few works have been reported that examine the separation of microalgae [34-36], particularly based on their intracellular lipid content [34, 35]. Microalgal cells can experience different magnitudes of nDEP or pDEP force depending on their lipid content [37, 38], resulting in different flow trajectories and thus, separation. Although DEP-based microfluidic devices have been successfully used to separate microalgal cells based on their intrinsic properties, only simple operations and applications such as separating two known microalgal strains with known lipid contents have been shown so far, and no real library screening work has been reported. In addition, no DEP-based microfluidic device exist that can accurately determine the intracellular lipid quantity beyond simple binary determination and separation (i.e., lipid vs no lipid, or high-lipid vs low-lipid). Last, these devices require relatively complicated and rather expensive experimental setups to generate the pDEP force at high-frequency (~50 MHz) and high-voltage (~30 V peak to peak (V_{PP})) [34, 35].

In this report, we present a lateral DEP-based microfluidic platform capable of separating cells based on their intracellular lipid content, which was exploited to monitor and quantify the heterogeneous distribution of intracellular lipid level of a given microalgal cell population, all label-free and at single-cell resolution. In addition, for the first time, real library screening was conducted using the platform, which was successfully demonstrated by obtaining high-lipid-producing microalgal populations and strains through multiple rounds of cell population enrichment steps, with and without chemical mutations in between each round.

2. Working principle

When electric field is induced with a planar interdigitated electrode array in a microchannel, the electric field gradient is strongest at the edge of the electrode, which can generate pDEP force acting on microalgal cells. Here, the electric field was calculated based on a line charge model [30]. When the interdigitated electrode array is positioned at an angle of θ to the flow direction (instead of the typical 90-degree angle, i.e., perpendicular to the flow direction), pDEP force is created around the electrode edges and attracts cells. Since the electrodes are angled, the attracted cells move along the flow direction while remaining attracted to the electrodes, and thus move not only along the flow direction but also laterally (Fig. 1). Due to the hydrodynamic force, the x-directional pDEP force (F_{DEP}) cannot hold onto the cells for too long, thus the cells are eventually released from the electrodes and move along the flow direction again, where they are caught by the next angled electrodes and continue the lateral movement. This lateral displacement of cells, $\Delta y'$, can be calculated by using the numerical simulation [31, 39] of:

$$\frac{d(\Delta y')}{dt} = \frac{F_{DEP}\cos\theta}{12\eta(S/l)} = \frac{\varepsilon_m V_c \cos\theta\, Re[f_{CM}] v_a^2}{32\eta\left(\frac{S}{l}\right)[\ln(8d/\pi a)]^2}\frac{\partial\left|\vec{A}\right|^2}{\partial x}, \qquad (1)$$

$$\vec{A} = \sum_{n=1}^{\infty}\left\{(-1)^{n+1}\frac{[x+(-1)^n(2n-1)d]\overrightarrow{a_x} + z\overrightarrow{a_z}}{[x+(-1)^n(2n-1)d]^2+z^2} + (-1)^{n+1}\frac{[x-(-1)^n(2n-1)d]\overrightarrow{a_x} + z\overrightarrow{a_z}}{[x-(-1)^n(2n-1)d]^2+z^2}\right\}$$

The symbols used in equation (1) are described in Appendix I. Here, the lateral displacement of microalgal cells strongly depends on the magnitude of pDEP force, which is proportional to the real part of the

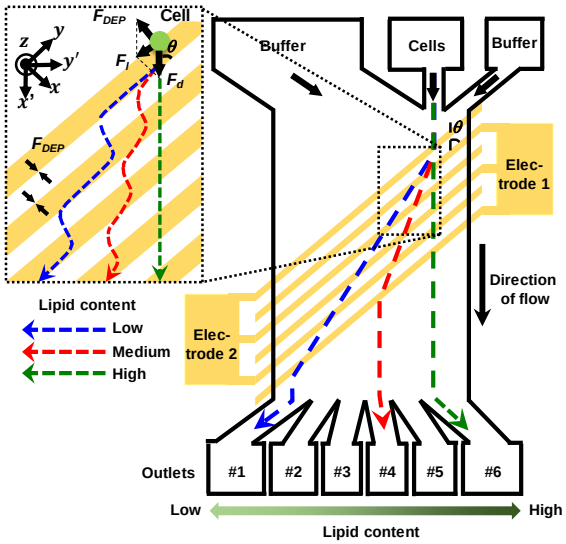

Fig. 1. Illustration of the lateral DEP microfluidic platform with a planar interdigitated electrode array is placed at an angle (5.7°) to the direction of the flow. The inset shows an enlarged view of the illustrative lateral movement of microalgal cells having different lipid level when passing over the electrode array where the pDEP force is generated. The channel width of the outlet #1-#5 is 300 µm, except for the outlet #6 (500 µm).

Clausius-Mossotti factor ($Re[f_{CM}], f_{CM} = \frac{\varepsilon_c^*(\omega)-\varepsilon_m^*(\omega)}{\varepsilon_c^*(\omega)+2\varepsilon_m^*(\omega)}, \varepsilon^* = \varepsilon - j\frac{\sigma}{\omega}$)) determined by the dielectric properties of cells and the surrounding media. In the case of microalgal cells producing intracellular lipid, their dielectric properties, which correlate with the cytoplasm conductivity (σ), are mostly affected by the cell's lipid level, as lipid has vastly different conductivity compared to the rest of the cytoplasm (mostly conductive saline solution). The cytoplasm conductivity of microalgal cells without lipid was previously reported to be around 0.5 S/m [34]. We hypothesized that the cytoplasm conductivity can be altered based on the volume fraction of intracellular lipid in cell's entire cytoplasm. Thus, this cytoplasm conductivity is expected to decrease from 0.5 to 0.4, 0.25, and 0.1 S/m as intracellular lipid level increases from 0 to 20, 50, and 80% of cell volume, respectively. Simulation using equation (1) shows that the real part of the Clausius-Mossotti factor decreases from 0.39 to 0.37, 0.32, and 0.17, respectively (surrounding media conductivity set to 0.04 S/m), at 3 MHz frequency (Fig. S1). Thus, when intracellular lipid level of a microalgal cell increases, pDEP force decreases. In this simulation, the diameter of microalgal cells was set to 7.6 µm (7.6 ± 0.6 µm, measured from 1,000 *Chlamydomonas reinhardtii* (*C. reinhardtii*) cells.

The x-directional pDEP force and lateral displacements were calculated using equation (1) with the different cytoplasm conductivities of 0.5, 0.4, 0.25, and 0.1 S/m when a microalgal cell passes over a single electrode (Fig. S2). If the cell has no intracellular lipid (σ=0.5), the pDEP force is larger than the hydrodynamic drag force, and the lateral displacement becomes infinite (i.e., displaced all the way to the end wall of the microfluidic channel). When the cytoplasm conductivities changed to 0.4, 0.25, and 0.1, where the magnitude of pDEP force at the edge of the electrodes decreased, the calculated lateral displacements per single electrode were 27, 24, and 4 µm, respectively. In other words, more lipid-producing cells have reduced cytoplasm conductivity, thus resulting in decreased their lateral displacement. This allows microalgal cells to be separated using the presented lateral DEP design purely based on their lipid level without any labelling requirement.

From the above equation (1), the size of microalgal cells is another factor that can affect the pDEP force applied to cells. Fig. S3(a-b) show that in the case of microalgal cells without lipid or with only small amount of lipid, the lateral displacement is dominated by the size of the cells. However, since their lateral displacement per single electrode is over 50 µm, most cells eventually reach the microfluidic channel wall and nowhere to move further. Thus, microalgal cells with very low intracellular lipid content can be pushed to one side of the microchannel regardless of their size variation. On the other hand, Fig. S3(c-d) show that when the cytoplasm conductivities changed from 0.25 to 0.1, the calculated lateral displacements were 24 ± 3 and 3.6 ± 0.1 µm, respectively. This means that as the amount of intracellular lipid increase, the lateral displacement is dominated by cytoplasm conductivity rather than size, which allows microalgal cells to be separated depending on their lipid level. In this work, we utilized this principle to design and fabricate a lateral DEP-based microfluidic platform, and utilized it for both digital quantification of algal lipid in a given population as well as conducting an iterative high-lipid-producing cell enrichment and separation assay.

3. Materials and methods

3.1 Design

The lateral DEP-based microfluidic sorting platform was designed to have three inlets, one for sample and the other two for buffer solutions, six outlets for collecting separated cells, and a planar interdigitated electrode array placed at an angle of 5.7° to the flow direction (Fig. 1). The width and spacing of the electrode array are both 30 µm. The height of the microchannel is set to 30 µm to minimize the variation of the pDEP force acting on microalgal cells along their vertical position. When microalgal cells are injected into the platform, they are focused into a 50 µm wide streamline by sheath flow from the two side buffer inlets. The focused cell streamline is formed around 300 µm away from the right-side microchannel wall. Since the channel width of the outlet #6 is 500 µm, all cells that are not influenced by the pDEP force (i.e., cells with very high intracellular lipid) will come out of outlet #6 (green dashed line in Fig. 1). Cells with the lowest intracellular lipid level (i.e., highest pDEP force) will experience the largest lateral displacement, and thus move towards outlet #1 (blue dashed line).

3.2 Microfluidic device fabrication

The lateral DEP microfluidic platform was made of a polydimethylsiloxane (PDMS) microchannel on a 0.7 mm thick borosilicate glass substrate with patterned DEP planar electrodes (Fig. S4). First, the angled planar electrode array was prepared by Cr/Au (20nm/100nm) deposition on the glass substrate, followed by conventional photolithography and selective Cr/Au etching. A 30 µm thick layer of SU-8 2025 photoresist (Microchem, USA) was patterned on a 3-inch silicon wafer to create the master mold for the microchannel. The SU-8 master mold was coated with Tridecafluoro-1, 1, 2, 2-Tetrahydrooctyl-1-Trichlorosilane (United Chemical Technologies, Inc., Bristol PA) to facilitate PDMS replication, followed by PDMS microchannel replication (10:1 mixture, Sylgard 184, Dow Corning, Inc., MI). After oxygen plasma treatment of both the electrode-patterned glass substrate and the PDMS replica, they were aligned and bonded together for 24 hr at 80°C.

3.3 Cell preparation

C. reinhardtii strain CC-406 (wall-deficient mutant, no motility) was used to characterize the performance of the developed platform. Unless otherwise stated, cells were cultured in Tris-Acetate-Phosphate (TAP) media at 22°C under continuous illumination (60 µmol photons/m^2·sec). CC-406 cells were collected during exponential growth phase (~10^6 cells/ml, typically after four days of culture), centrifuged at 600 g (1900 rpm) for 5 min, and resuspended in TAP media lacking NH_4Cl (TAP-N) with a concentration of 2×10^7 cells/ml. Four different CC-406 samples with different lipid content were prepared by cultivation in TAP-N media for different incubation durations (12, 24, 36, and 48 hours).

In order to achieve DEP-based cell separation, all samples were resuspended in low conductivity media (0.04 S/m) before using the cells in the developed microfluidic platform. The low conductivity media contains 2.7 mM of potassium chloride (P9333, Sigma-Aldrich, USA), 0.3 mM of monopotassium phosphate (1551139, Sigma-Aldrich, USA), 0.85 mM of dibasic potassium phosphate (1151128, Sigma-Aldrich, USA), 280 mM of myo-Inositol (I5125, Sigma-Aldrich, USA), suspended in de-ionized (DI) water, and then filtered by using a 0.2 µm membrane before use.

3.4 EMS mutagenesis

Ethyl methanesulfonate (EMS) mutagenesis was conducted as described in previous studies [15, 27]. Briefly, CC-406 cells were grown to an OD_{750} of 0.6 (5×10^6 cells/ml), centrifuged, and resuspended in 6 ml of TAP media containing 225 mM of EMS. Sample tubes were wrapped with aluminium foil and incubated at room temperature for 80 min using a rocking table. After incubation, cells were harvested

by centrifugation and the pellets were washed three times with 12 ml of TAP media. Cells were then resuspended in 6 ml of TAP media and stored for cell recovery in dark for 15-18 hr. This procedure was optimized to have an approximate killing rate of 80% from EMS treatment (number of dead cells counted through Evans Blue staining); a condition typically deemed to have sufficient mutation in the population [27]. The final step prior to sample loading into the lateral DEP microfluidic platform was centrifugation, resuspension in TAP-N media, and dilution to a concentration of 2×10^7 cells/ml, followed by 72 hr incubation for lipid induction.

3.5 On-chip lateral DEP separation

Three syringe pumps provided controlled flow through the microchannel. Two syringe pumps were used respectively to push the cell sample and two buffer solutions into the microchannel. The other syringe pump was used to withdraw six syringes, each connected to the six outlets, and functioned as a reservoir to collect the separated cells. The sample and buffer flow rate were 10 µl/hr and 140 µl/hr, respectively, thus the total volumetric flow rate was 150 µl/hr. To match the total flow volume, the withdraw flow rate of each outlet was set to 22.5 µl/hr, except for outlet #6 that was wider (set at 37.5 µl/hr). Subsequently, microalgal cells were flown through the device, collected from each outlet, and stained with BODIPY (Boron-dipyrromethene) to quantify the intracellular lipid content [40, 41]. To generate pDEP force, 3 MHz, 5-9 V_{PP} sinusoidal voltage was supplied from a function generator (DG4202, Rigol Technologies Inc.). For device characterization, 3 MHz, 5-6 V_{PP} sinusoidal waves were applied to the device. The iterative screening process using natural and chemically mutated populations was conducted under 3 MHz, 9 and 7 V_{PP} sinusoidal wave, respectively. A Zeiss Axio Observer Z1 microscope (Carl Zeiss Micro Imaging, LLC) was used to count the number of microalgal cells flowing through the microchannel using chlorophyll autofluorescence (excitation: 460-500 nm, emission > 610 nm). About 1,000 cells were analyzed to obtain each lateral distribution graph.

3.6 Off-chip lipid content analysis

The lipid content of the separated cells collected from each outlet was further analyzed through an off-chip lipid staining and analysis step. Neutral lipid straining fluorescent dye BODIPY was used, where 1 ml of cell sample was mixed with 10 µl of BODIPY stock solution (0.5 mg/ml in DMSO), incubated for 10 min in dark, and rinsed at least 3 times with fresh TAP media. Both fluorescence microscopy and flow cytometry were conducted to analyze the lipid content. For fluorescence microscopy, BODIPY fluorescence (excitation: 460-500 nm, emission: 500-550 nm) of retrieved cells from each outlet was measured. About 50 cells were analyzed for each measurement. All microscopic images were analyzed with the NIH Image J software. For flow cytometry, a 488 nm laser was used to excite BODIPY fluorescence and detected at 525 ± 25 nm (BD FACSAria II Cell Sorter). The flow cytometer measurement was considered complete when the total number of analyzed cells reached 10,000. Data was analyzed by FlowJo software (TreeStar, San Carlos, CA, USA) and the average BODIPY fluorescence intensity of each mutant was analyzed and presented as a histogram (Fig. 3c and S6).

4. Results

4.1 Lateral displacement of cells based on their intracellular lipid content

C. reinhardtii strain CC-406 (cw15), known to accumulate intracellular lipid under stressed conditions such as nitrogen

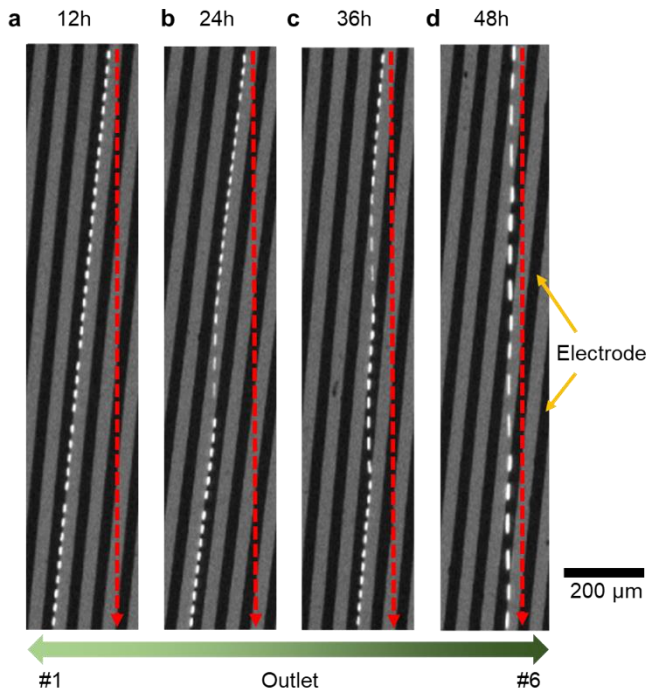

Fig. 2. Fluorescence microscopy images of CC-406 cell trajectories (white line) inside the lateral DEP device. Cells cultured in TAP-N media for (a) 12 (b) 24 (c) 36, and (d) 48 hr showed different trajectories compared to the direction of the flow (red line, straight).

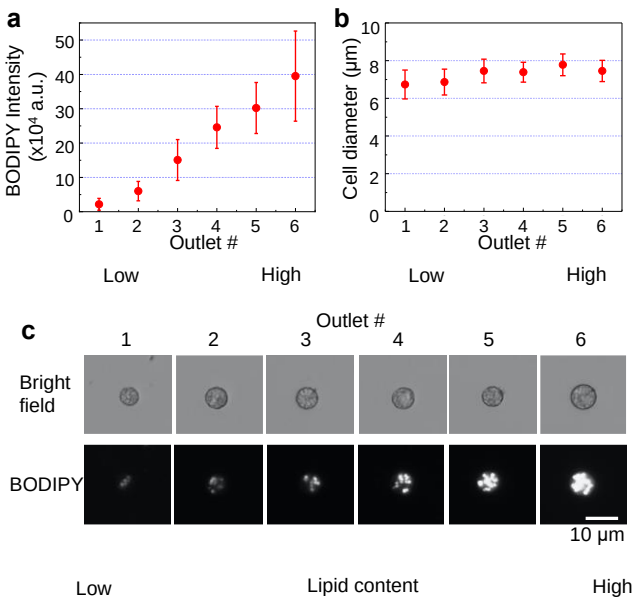

Fig. 3. Efficiency of separating cells based on their different intracellular lipid level using the lateral DEP microfluidic platform (applied voltage: 3 MHz, 5 V_{pp} sinusoidal wave). (a) Measured average BODIPY fluorescence intensities of CC-406 cells (n=56, ± SD) collected from each outlet. (b) Average size of cells (n=56, ± SD) collected from each outlet. (c) Representative microscopy images of cells collected from each outlet.

starvation [42], was cultured in TAP-N media for 12, 24, 36, and 48 hr to induce intracellular lipid to a different degree [43]. More intracellular lipid level was observed from longer nitrogen-stressed samples, analyzed through fluorescent neutral lipid BODIPY staining and flow cytometry (Fig. S7). To confirm the operation of the lateral DEP microfluidic platform, CC-406 cells cultured in TAP-N media for 12 hr were tested. All cells were separated into outlet #6 when no DEP voltage was applied (video 1(a)), while most cells were separated into outlet #1 when applying a DEP voltage of 6 V_{PP} at 3 MHz (video 1(b)).

The feasibility of the lateral DEP microfluidic platform to separate microalgal cells that have different lipid level was evaluated in two ways: comparison of trajectories of lateral displacement in the microfluidic channel, and comparison of lipid level of cells collected from each of the six outlets. When CC-406 cells with no lipid passed over the planar electrode array, most of them were trapped on the electrode edge when applying a DEP voltage of 5 V_{PP} at 3 MHz. Trajectory analysis (Fig. 2(a)) showed that CC-406 cells with small amount of lipid (12 hr incubation) had an average lateral displacement of 145.9 ± 72.9 µm per single electrode, and continuously moved along the edge of the electrode, eventually being separated into outlet #1. Cells with higher level of lipid content (24, 36, and 48 hr incubation) showed average lateral displacements of 67.9 ± 30.7, 36.0 ± 22.2, and 8.6 ± 3.4 µm per single electrode, respectively (Fig. 2(b-d)). This result clearly indicates that the amount of lateral displacement is directly influenced by the intracellular lipid level of cells.

Next, to further provide quantitative data on the cell separation capability of the microfluidic device based on cell's intracellular lipid level, the lipid content of the cells collected from each outlet were analyzed through BODIPY staining. Fig. 3(a) shows the average BODIPY fluorescence intensities of the cells collected from outlet #1 through outlet #6, which increased from 2.2 ± 1.7 to 6.0 ± 2.8, 15.1 ± 6.0, 24.6 ± 6.1, 30.2 ± 7.4, and 39.5 ± 13.1 ($\times 10^4$ a.u.), respectively. This means that cells with higher lipid level have less lateral displacement (move towards outlet #6), while cells with lower lipid level has larger lateral displacement (move towards outlet #1). BODIPY fluorescence intensity of cells collected from each outlet all showed statistical difference tested through independent-samples t-test ($n = 56$, $p < 2.7\times10^{-5}$). To check whether cell size variation may have influenced the DEP lateral displacement result, average cell sizes from each outlet were measured. However, no significant differences in cell sizes between each outlet were observed Fig. 3(b). Fig. 3(c) shows representative microscopy images of cells collected from each outlet. Taken together, this result confirmed that the developed lateral DEP microfluidic platform can digitally quantify and separate cells based on their intracellular lipid level.

4.2 Control of lateral distribution of cells through DEP voltage control

Lateral distribution of cells separated through the developed device (i.e. percentage of cells separated into each outlet) represents the distribution of cells having different intracellular lipid level in a given population. Fig. 4(a) (top row) shows such distributions when a DEP voltage of 5 V_{PP} was applied. It was observed that as the population shifts from 12 hr (left) to 48 hr (right) incubation in N-limited culture (i.e., from less to more lipid-producing population), more cells came out of outlet #6 rather than from outlet #1. The degree of this distribution can be altered by simply adjusting the applied voltage so that only a very small fraction of cells that show the highest lipid content comes out of outlet #6. Fig. 4(b) and 4(c) show how the lateral distribution of the same CC-406 cell population changes under the different voltage conditions of 5, 5.5, and 6 V_{PP}. Comparing the lateral distribution along each column, as the applied voltage increased, more cells were observed coming out of outlet #1 (distribution profile moving from right to left), while less cells came out of outlet #6. This simple voltage control allowed controlling the sorting threshold based on cell's intracellular lipid level. For example, when a DEP voltage of 5 V_{PP} was applied, 83% of cells that were cultured in TAP-N media for 48 hr was collected from both outlets #5 and #6. By increasing the applied voltage to 5.5 and 6 V_{PP}, this percentage dropped to 44% and 19%, respectively. When counting cells from only outlet #6 (e.g., for enrichment applications), the percentage dropped to 2 and 1.6%, respectively (from 23%, when a voltage of 5 V_{PP} was applied). This result clearly demonstrated the capability of the platform to control the percentage of cells separated into each outlet by simply adjusting the applied voltage. This is particularly advantageous when wanting to only select the highest lipid-producing microalgal cells in a given population.

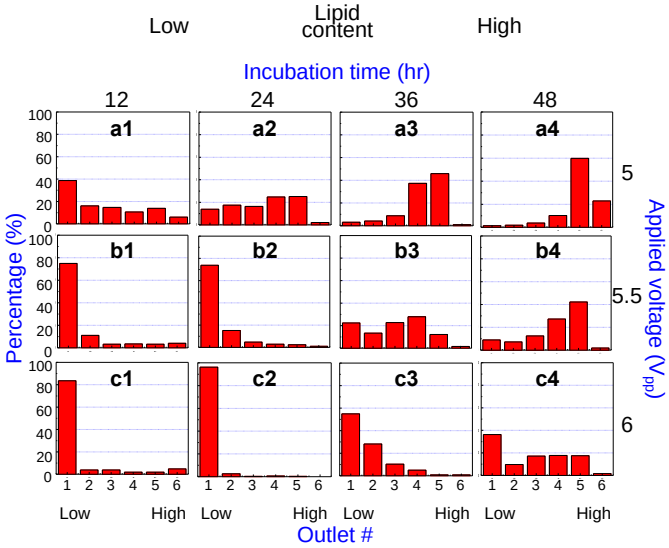

Fig. 4. The lateral distributions of CC-406 cells cultured in TAP-N media for 12 hr (a1, b1, c1), 24 hr (a2, b2, c2), 36 hr (a3, b3, c3), and 48 hr (a4, b4, c4) were obtained by calculating the percentage of cells separated into each outlet. The effect of different DEP voltages applied on the lateral distributions were also tested: (a1-4) 5 V_{pp}, (b1-4) 5.5 V_{pp}, and (c1-4) 6 V_{pp}.

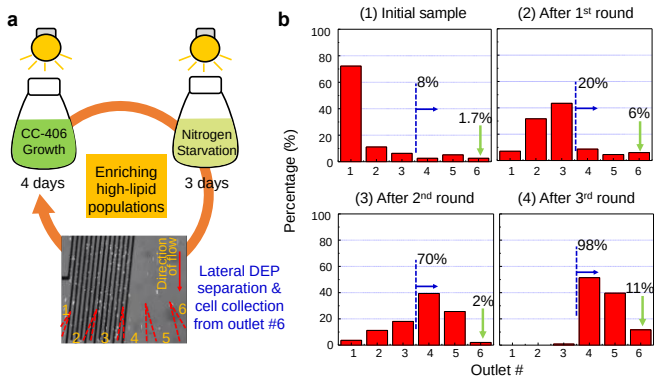

Fig. 5. (a) Illustration showing the iterative high-lipid-producing cell enrichment and selection process. (b1) Lateral distributions of wild-type CC-406 cells of the starting population; (b2) after round 1; (b3) after round 2; (b4) after round 3. The applied voltage was 3 MHz, 9 V_{pp}.

4.3 Enrichment of high-lipid-producing *C. reinhardtii* cells

As a first real screening application, the developed platform was used for conducting three rounds of enrichment process from wild-type CC-406 populations to obtain a population that has a larger number of high-lipid-producing cells. Fig. 5(a) shows the iterative experimental procedure of this enrichment process; 1) cell growth in TAP media for 4 days to obtain enough cells, 2) cell incubation in TAP-N media for 72 hr for intracellular lipid induction and accumulation, 3) selection of high-lipid-producing cells through the developed platform (separation and collection from only outlet #6), 4) repeat steps #1 to #3. During the enrichment process, the lateral distribution of cells in each round was monitored and compared to analyze how the overall cell population changed (Fig. 5(b)). From the initial population, the DEP voltage was adjusted to 9 V_{PP} so that only 1.7% of cells from the starting population were collected from outlet #6 (Fig. 5(b-1)). Cells coming out of outlets #4 to #6 are all deemed to be relatively high-lipid producers, occupying 8% of the overall population. Approximately 3,000 cells were collected from outlet #6 over a 3-hr period, and then re-cultured in TAP media to expand the population. After this first round of enrichment, cells coming out of outlets #4 to #6 combined together increased to 20%, and the percentage of cells coming out of outlet #6 was 6% (Fig. 5(b-2)).

For the 2nd and 3rd rounds of the microfluidic chip-based enrichment process, the percentages of cells coming out of outlet #6 were 2% and 11%, respectively, while the percentages of cells coming out of outlets #4 to #6 were 70% and 98%, respectively (Fig. 5(b3-4)). Overall, the lateral distribution profiles progressively moved from outlet #1 to #6 where the fraction of cells separated into outlet #4 to #6 gradually increased over the rounds, from 8% (initial sample), to 20, 70 and 98% (3rd round), respectively. To further confirm that we are indeed enriching the cell population to have higher lipid content, BODIPY lipid staining followed by fluorescence intensity analysis were carried out after each round. The average BODIPY fluorescence intensities of the starting population and samples from each round of enrichments were 37 ± 10.9, 40.4 ± 11.8, 43.4 ± 10.5 and 56.1 ± 9.8 (× 10^4 a.u.), respectively, meaning that the overall population indeed shifted to have higher number of high-lipid-producing cells. Here, the average BODIPY intensity of the 3rd round enrichment population is about 1.5 times higher than that of the starting population.

4.4 Screening of EMS-mutagenized *C. reinhardtii* library for selecting high-lipid-producing mutants

Following the success in enriching a starting population to contain higher percentage of high-lipid-producing cells, we next applied the platform to iteratively select high-lipid-producing mutants from a chemically mutated *C. reinhardtii* library. The motivation for conducting such an assay is because enrichment of a population may not necessary result in stable strains that show high lipid production, as the natural mutation rates of cells are quite low [13, 14]. Thus, here a random mutagenesis strategy was applied to CC-406 cells through EMS treatment to generate a mutant library. The developed platform was then used to select high-lipid-producing strains using a similar selection procedure described in the previous section.

Fig. 6(a) shows the lateral distribution of the starting population, where 8.8% of the cells came out of outlets #4 to #6 combined, and only 1.8% from outlet #6. From here, cells coming out of outlet #6 were collected, diluted, and put on agar plates with dilution to form multiple single colonies. Twelve of these single colonies were randomly picked, each cultured in TAP media and expanded, followed by resuspension in TAP-N media for 72 hr to induce lipid. Off-chip lipid characterization was conducted using flow cytometry combined with BODIPY staining (Fig. S5). Among the 12 mutants, mutant #5 (marked as 1st-mutant #5) showed the highest average BODIPY intensity, which was 1.4 times higher (1262 ± 520 (a.u.)) compared to that of wild-type CC-406 cells (914 ± 498 (a.u.)), and thus selected for another round of subsequent selection process. The characteristics of the mutant #5 was further analyzed by the lateral DEP microfluidic platform (Fig. 6(b)). When comparing the lateral distribution profiles of wild-type CC-406 and the 1st-mutant #5 cells (Fig. 6(a-b)), the proportion of cells coming out of outlets #4 to #6 combined changed from 8.8 to 41.7%, respectively, clearly showing that this can be a promising strategy in selecting high-lipid-producing mutants.

Next, another round of mutation and selection process was applied to the re-cultured mutant #5. The 1st-mutant #5 cells underwent another round of EMS treatment, and then screened through the microfluidic device. Again, cells collected from outlet #6 were plated on agar plates to form multiple single colonies. From here, 22 colonies were randomly selected, and then analyzed by flow cytometry. Based on the histogram analysis, the 2nd-mutant #2, 8, 13, 15, 16, and 17 all showed over 1.3 times higher average BODIPY intensity than that of the wild-type CC-406 cells (1388 ± 716 (a.u.)) (Fig. S6). Among them, the 2nd-mutant #16 showed the highest average BODIPY intensity, which was 1.6 times higher (2232 ± 942 (a.u.)) compared to that of wild-type CC-406, and thus was selected for further analysis. Overall, when comparing the lateral distribution profiles of the population, the portion of cells coming out of outlets #4 to #6 combined were 8.8, 41.7 and 58.9% for wild-type CC-406, 1st-mutant #5, and 2nd-mutant #16 cells, respectively (Fig. 6(a-c)). In summary, seven potentially promising high-lipid-producing microalgal strains were found through the use of the developed lateral DEP microfluidic platform, which is now undergoing further down-stream analysis.

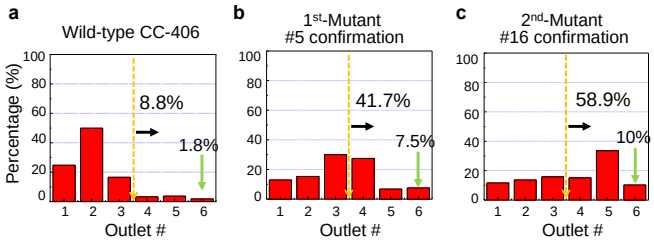

Fig. 6. Lateral displacement of (a) wild-type CC-406 cells, (b) 1st-Mutant #5, and (c) 2nd-Mutant #16. The applied voltage was 3 MHz, 7 V_{pp}.

5. Discussion

This paper presents a lateral DEP-based microfluidic sorting platform that allows for 1) providing digital quantification of the intracellular lipid level of a given microalgal cell population, 2) selecting cells/strains that show enhanced lipid production, and 3) enriching a given population to have more high-lipid-producing cells. The pDEP force acting on the cells is inversely proportional to their lipid level, resulting in different degree of lateral displacements (i.e., more lipid ➔ less pDEP force applied ➔ less lateral displacement). Based on this principle, the developed platform successfully separated microalgal cells with different lipid levels into the six cell collection outlets and could be employed to actually provide a profile of the intracellular lipid level of a given population in real-time.

Another distinguishing feature of the developed platform is that the applied voltage can be readily adjusted to collect only the top few percent of cells in terms of their intracellular lipid level in a given population, which was demonstrated by adjusting the voltage so that less than 2% of the top lipid producers from a given population could be sorted and collected. This allowed an iterative enrichment process to be conducted under a stringent selection condition to enhance the possibility of obtaining potential variants having high lipid production capability. These capabilities were not available in previously developed DEP-based microalgae cell separation microfluidic systems [34, 35].

The presented platform has another advantage, where the operation conditions for the DEP separation function were at a much lower frequency and voltage range (3 MHz, 5-9 V_{PP}), compared to the previously reported DEP-based microalgae separation platforms (e.g., 50 MHz, 30 V_{PP}) [34, 35]. Since this low frequency and low voltage signal can be easily generated using a generic low-cost function generator, the developed platform can eliminate the need for expensive high-end instruments, which enables broader utilization of such a device. Also, this low voltage can reduce potential cell damages resulting from the high-intensity electric field near the electrode edges as well as joule heating [44, 45]. In the presented work, the calculated maximum electric field in the device was 85 kV/cm at 9 V_{PP}, an electric field strength known to have little effect on cell viability. This was verified through Evans blue staining of cells flowing through the microfluidic system, where 98% of the cells screened through the microfluidic platform showed good viability (compared to 99% for the initial cell population), indicating that the applied low voltage has no negative impact on cell viability.

The optimized sample flow rate was 10 µl/hr to effectively apply the DEP force on cells (cell concentration: 2×10^7 cells/ml), meaning that the throughput of the single-channel lateral DEP microfluidic channel was 20 cells/sec. Previous DEP-based microalgae separation study reported a maximum throughput of 10^3 cells/sec [35]. Although this previous system showed higher throughput, this device simply separated microalgal samples into two groups, high- and low-lipid producing cells, which did not require high separation resolution. Although the throughput of the presented device is lower compared to the previous study, the device can provide a precise and accurate profile of the intracellular lipid amount of microalgal cells in a given population. In addition, the platform allows for obtaining the accurate lipid distribution profile of 1,000 microalgal cells within 50 min, capable of providing rapid real-time monitoring of the lipid level of a given population. If a higher throughput is needed, a multi-channel approach can readily achieve any needed throughput.

Current state of the art cell identification and separation tools such as FACS have been utilized to discover high-lipid-producing microalgal variants at high throughput and single-cell resolution (>10^3 cells/sec) [15-17]. However, staining process using Nile red and BODIPY is required, which results in significantly lower cell viability as well as requires additional sample preparation steps. On the other hand, the developed DEP-based platform can select microalgal cells showing high-lipid production without any labelling step, thus the negative effects of cell staining can be avoided. Also, compared to the active sorting method of FACS, the cell collection method where just a constant flow of samples is required makes the overall instrument requirement very simple, making this microfluidic device potential for a field-deployable system. In terms of cost burden, a FACS instrument and its maintenance are relatively expensive, typically housed in central user facilities. However, a DEP-based microfluidic setup costs less than $500, with material cost of a reusable single-chip being less than $30, making this a highly attractive solution.

Adaptive laboratory evolution (ALE) has been carried out to improve microalgal attributes through long-term selection of serial dilution in normal TAP media [46, 47] and under the abiotic stresses such as high CO_2 [48], salt concentrations [49, 50], light intensity [51, 52], temperature [53], and cooperative multi-factors [54]. Although useful, this process is quite time-consuming. For example, Yu et. al. [46] discovered strains having 1.5 times faster growth rate and 1.2 times higher lipid accumulation than the starting cells, however the overall process took 28 serial dilution cycles over a 84 day period. Also, populations having 1.35 times faster growth rate than the initial population were found after 1,880 generations selected over 17 months [47]. Compared to this, a single round of ALE process using the developed lateral DEP microfluidic platform was completed within a week, with most of the time spent to simply regrow the selected cells (3 hr of on-chip selection process, followed by 96 hr of cell re-growth to create the starting population for the next round of ALE). Through three iterative ALE processes, a population having 1.5 times higher lipid production compared to the initial sample was successfully obtained, significantly shorter than previously reported methods. Thus, we expect that this approach has the potential to significantly decrease the time required for ALE assays.

The developed lateral DEP-based microfluidic sorting platform carried out the assays using only one microalgal species, *C. reinhardtii*. However, there is no limitation on the type of unicellular microalgal cells that can be used in this platform, such as *Chlorella* sp. [48], *Nannochloropsis* sp. [50], *Synechocystis* sp. [53], *Schizochytrium* sp. [54], all being microalgae of high interest for lipid production. However, whether non-spherical cells can also be separated purely based on their intracellular lipid level remains to be seen (planned future studies), where such cell's movement could be influenced by different hydrodynamic force.

Microalgae including CC-406, *Chlorella. vulgaris*, *dw15*, and *pgd1*, which have been used as model samples in previously developed DEP-based sorting systems [34, 35], can accumulate lipid as well as starch [55] which also has high dielectric constant. Regardless of starch accumulation in TAP-N cultivation, microalgae experienced different DEP force and could be separated depending on their lipid level, which was successfully demonstrated based on BODIPY fluorescence intensity. In future work, starch-less mutant, for example *C. reinhardtii* strain *star6*, can be used in this DEP-based platform to show how accumulated starch may affect microalgae separation.

As a further downstream analysis, the growth rate of the 1st-mutant #5 and the 2nd-mutant #16 were analysed and showed that their growth rate was not significantly different from that of control (Fig. S8). Here, EMS chemical random mutagenesis strategy was utilized, but other physical mutagenic methods such as UV light, gamma ray, and X-ray can be used as alternative methods [56]. Also, instead of the fluorescent lipid staining method, lipid level of strains discovered can be further analysed through gravimetric quantification, high-performance liquid chromatography (HPLC), or near infrared (NIR) spectroscopy once a large-scare cultivation is achieved [57].

In the future, the developed platform can be further improved by integrating impedance-based cell counting technology [58-61], which can characterize the number of cells flowing through each outlet automatically, making the analysis process easier. Such a fully automated system will be capable of conducting real-time analysis of microalgal cell population to determine their lipid content.

Conclusion

The developed platform has the capability to sort cells based on the degree of their intracellular lipid level, somewhat similar to using

fluorescence intensity of fluorescent lipid-stained cells. The platform has broad application perspective, which not only includes obtaining high-lipid-producing strains or enrichment of a given population, but also to rapidly assess the heterogeneity of intracellular lipid level to making best harvesting decisions during algal biofuel production. The present setup, including the device, is relatively cheap and easy to build, thus it can be integrated also into a portable system, which would enable real-time onsite monitoring and screening in large scale microalgal culture systems.

Conflicts of interest

There are no conflicts to declare.

Acknowledgements

This work was supported by the National Science Foundation (NSF) Emerging Frontiers in Research and Innovation (EFRI) grant #1240478. Any opinions, findings, and conclusions or recommendations expressed in this material are those of the author(s) and do not necessarily reflect the views of the National Science Foundation.

Notes

Author contributions

S.-I.H., H.S.K., and A.H. designed the experiments and co-wrote the manuscript. S.-I.H. performed the experiments. K.-H.H helped with the theoretical analysis. A.H. supervised the work and wrote the manuscript.

APPENDIX I. NOTATION

The following symbols are used in this paper:

ε_c^* = complex permittivities of microalgae
ε_m^* = complex permittivities of suspension media
ε = permittivity of the material
σ = electrical conductivity of the material
t = time
η = apparent viscosity of microalgal cell in a suspension media
S = maximum cross-sectional area
l = characteristic length of microalgal cell
a = effective radius of the electrode
d = half width and half spacing of a planal interdigitated electrode
F_{DEP} = x-directional pDEP force
$Re[f_{CM}]$ = real part of the Clausius-mossotti factor
V_c = microalgal cell volume
v_a = applied voltage
$\vec{A}$ = calculated electric field
x = x-directional cell position ($-d/2 < x < d/2$)
z = levitation height of microalgal cell from the electrode array
$\overrightarrow{a_x}$ = x-directional unit vector
$\overrightarrow{a_z}$ = z-directional unit vector

References

1. G. Markou, D. Vandamme and K. Muylaert, *Water Research*, 2014, **65**, 186-202.
2. L. Zhu, *Renewable and Sustainable Energy Reviews*, 2015, **41**, 1376-1384.
3. T. M. Mata, A. A. Martins and N. S. Caetano, *Renewable and Sustainable Energy Reviews*, 2010, **14**, 217–232.
4. R. H. Wijffels and M. J. Barbosa, *Science*, 2010, **329**, 796-799.
5. S.-F. Han, W.-B. Jin, R.-J. Tu and W.-M. Wu, *Critical Reviews in Biotechnology*, 2015, **32**, 255-268.
6. A. Han, H. Hou, L. Li, H. S. Kim and P. d. Figueiredo, *Trends in Biotechnology*, 2013, **31**, 225-232.
7. X. Zeng, M. K. Danquah, X. D. Chen and Y. Lu, *Renewable and Sustainable Energy Reviews*, 2011, **15**, 3252-3260.
8. D. R. Georgianna and S. P. Mayfield, 2012, **488**, 329-335.
9. Y. Chisti, *Journal of Biotechnology*, 2013, **167**, 201-214.
10. I. Havlik, P. Lindner, T. Scheper and K. F. Reardon, *Trends in Biotechnology*, 2013, **31**, 406-414.
11. M. Hlavova, Z. Turoczy and K. Bisova, *Biotechnology Advances*, 2015, **33**, 1194-1203.
12. A. Ghosh, S. Khanra, M. Mondal, G. Halder, O. N. Tiwari, S. Saini, T. K. Bhowmick and K. Gayen, *Energy Conversion and Management*, 2016, **113**, 104-118.
13. X. Li, E. R. Moellering, B. Liu, C. Johnny, M. Fedewa, B. B. Sears, M.-H. Kuo and C. Benning, *The Plant Cell*, 2012, **24**, 4670-4686.
14. C. Yan, J. Fan and C. Xu, *Methods in Cell Biology*, 2013, **116**, 71-80.
15. B. Xie, D. Stessman, J. H. Hart, H. Dong, Y. Wang, D. A. Wright, B. J. Nikolau, M. H. Spalding and L. J. Halverson, *Plant Biotechnology Journal*, 2014, **12**, 872-882.
16. M. Terashima, E. S. Freeman, R. E. Jinkerson and M. C. Jonikas, *The Plant Journal*, 2015, **81**, 147-159.
17. K. Yamada, H. Suzuki, T. Takeuchi, Y. Kazama, S. Mitra, T. Abe, K. Goda, K. Suzuki and O. Iwata, *Scientific Reports*, 2016, **6**, 1-8.
18. H. S. Kim, T. L. Weiss, H. R. Thapa, T. P. Devarenne and A. Han, *Lab on a Chip*, 2014, **14**, 1415-1425.
19. H. S. Kim, T. P. Devarenne and A. Han, *Lab on a Chip*, 2015, **15**, 2467-2475.
20. J. Y. H. Kim, H. S. Kwak, Y. J. Sung, H. I. Choi, M. E. Hong, H. S. Lim, J.-H. Lee, S. Y. Lee and S. J. Sim, 2016, **6**, 21155.
21. B. Guo, C. Lei, H. Kobayashi, T. Ito, Y. Yalikun, Y. Jiang, Y. Tanaka, Y. Ozeki and K. Goda, *Cytometry Part A*, 2017, **91A**, 494-502.
22. H. S. Kim, T. P. Devarenne and A. Han, *Algal Research*, 2018, **30**, 149-161.
23. Y. Suzuki, K. Kobayashi, Y. Wakisaka, D. Deng, S. Tanaka, C.-J. Huang, C. Lei, C.-W. Sun, H. Liu, Y. Fujiwaki, S. Lee, A. Isozaki, Y. Kasai, T. Hayakawa, S. Sakuma, F. Arai, K. Koizumi, H. Tezuka, M. Inaba, K. Hiraki, T. Ito, M. Hase, S. Matsusaka, K. Shiba, K. Suga, M. Nishikawa, M. Jona, Y. Yatomi, Y. Yalikun, Y. Tanaka, T. Sugimura, N. Nitta, K. Goda and Y. Ozeki, *Proceedings of the National Academy of Sciences*, 2019, **116**, 15842–15848.
24. Y. J. Sung, H. S. Kwak, M. E. Hong, H. I. Choi and S. J. Sim, *Analytical Chemistry*, 2018, **90**, 14029-14038.
25. S. Abalde-Cela, A. Gould, X. Liu, E. Kazamia, A. G. Smith and a. C. Abell, *Journal of the Royal Society Interface*, 2015, **12**, 106.
26. H. S. Kim, A. R. Guzman, H. R. Thapa, T. P. Devarenne and A. Han, *Biotechnology and Bioengineering*, 2016, **113**, 1691-1701.
27. H. S. Kim, S.-C. Hsu, S.-I. Han, H. R. Thapa, A. R. Guzman, D. R. Browne, M. Tatli, T. P. Devarenne, D. B. Stern and A. Han, *Plant Direct*, 2017, 1-13.
28. B. Cetin and D. Li, *Electrophoresis*, 2011, **32**, 2410-2427.
29. C. Qian, H. Huang, L. Chen, X. Li, Z. Ge, T. Chen, Z. Yang and L. Sun, *International Journal of Molecular Sciences*, 2014, **15**, 18281-18309.

30. K.-H. Han and A. B. Frazier, *Lab on a Chip*, 2008, **8**, 1099-1086.
31. S.-I. Han, S.-M. Lee, Y.-D. Joo and K.-H. Han, *Lab on a Chip*, 2011, **11**, 3864-3872.
32. J. Jung, S.-K. Seob, Y.-D. Joo and K.-H. Han, *Sensors and Actuators B: Chemical*, 2011, **157**, 314-320.
33. T. Z. Jubery, S. K. Srivastava and P. Dutta, *Electrophoresis*, 2014, **35**, 691-713.
34. Y.-L. Deng, M.-Y. Kuo and Y.-J. Juang, *Biomicrofluidics*, 2014, **8**, 064120.
35. H. Hadady, D. Redelman, S. R. Hiibel and E. J. Geiger, *AIMS Biophysics*, 2016, **3**, 398-414.
36. Y. Wang, J. Wang, X. Wu, Z. Jiang and W. Wang, *Electrophoresis*, 2019, **40**, 969-978.
37. Y.-L. Deng, J.-S. Chang and Y.-J. Juang, *Bioresource Technology*, 2013, **135**, 137–141.
38. H. Hadady, J. J. Wong, S. R. Hiibel, D. Redelman and E. J. Geiger, *Electrophoresis*, 2014, **35**, 3533-3540.
39. K.-H. Han, S.-I. Han and A. B. Frazier, *Lab on a Chip*, 2009, **9**, 2958–2964.
40. T. Govender, L. Ramanna and F. B. I. Rawat, *Bioresource Technology* 2012, **114**, 507-511.
41. J. Rumin, H. Bonnefond, B. Saint-Jean, C. Rouxel, A. Sciandra, O. Bernard, J.-P. Cadoret and G. l. Bougaran, *Biotechnology for Biofuels*, 2015, **8**, 42.
42. Z. T. Wang, N. Ullrich, S. Joo, S. Waffenschmidt and U. Goodenough, *Eukaryotic Cell*, 2009, **8**, 1856-1868.
43. H. S. Kim, S. C. Waqued, D. T. Nodurft, T. P. Devarenne, V. V. Yakovlevb and A. Han, *Analyst*, 2017, **142**, 1054-1060.
44. X. Xuan, *Electrophoresis*, 2008, **298**, 33-43.
45. C. Church, J. Zhu, G. Huang, T.-R. Tzeng and X. Xuan, *Biomicrofluidics*, 2010, **4**, 044101.
46. S. Yu, Q. Zhao, X. Miao and J. Shi, *Bioresource Technology*, 2013, **147**, 499–507.
47. M.-M. Perrineau, J. Gross, E. Zelzion, D. C. Price, O. Levitan, J. Boyd and D. Bhattacharya, *PLOS One*, 2014, **9**, e92533.
48. D. Li, L. Wang, Q. Zhao, W. Wei and Y. Sun, *Bioresource Technology*, 2015, **185**, 269–275.
49. M.-M. Perrineau, E. Zelzion, J. Gross, D. C. Price, J. Boyd and D. Bhattacharya, *Environmental Microbiology*, 2014, **16**, 1755–1766.
50. C. H. Ra, C.-H. Kang, N. K. Kim, C.-G. Lee and S.-K. Kim, *Renewable Energy*, 2015, **80**, 117-122.
51. W. Fu, Ó. Guðmundsson, G. Paglia, G. Herjólfsson, Ó. S. Andrésson, B. Ø. Palsson and S. Brynjólfsson, *Applied Microbiology and Biotechnology*, 2013, **97**, 2395-2403.
52. C.-H. Ra, C.-H. Kang, J.-H. Jung, G.-T. Jeong and S.-K. Kim, *Bioresource Technology*, 2016, **212**, 254–261.
53. U. M. Tillich, N. Wolter, P. Franke, U. Dühring and M. Frohme, *BMC Biotechnology*, 2014, **14**, 1-15.
54. X. M. Sun, L. J. Ren, Z. Q. Bi, X. J. Ji, Q. Y. Zhao, L. Jiang and H. Huang, *Biotechnology for Biofuels* 2018, **11**, 1-16.
55. M. Siaut, S. p. Cuiné, C. Cagnon, B. Fessler, M. Nguyen, P. Carrier, A. Beyly, F. Beisson, C. Triantaphylidès, Y. Li-Beisson and G. Peltier, *BMC Biotechnology*, 2011, **11**, 7-21.
56. W. Fu, A. Chaiboonchoe, B. Khraiwesh, D. R. Nelson, D. Al-Khairy, A. Mystikou, A. Alzahmi and K. Salehi-Ashtiani, *Marine drugs*, 2016, **14**.
57. Y. Han, Q. Wen, Z. Chen and P. Li, *Energy Procedia*, 2011, **12**, 944-950.
58. S.-I. Han, Y.-D. Joo and K.-H. Han, *Sensors and Actuators B: Chemical*, 2012, **171-172**, 1312-1320.
59. S.-I. Han and K.-H. Han, *Analytical Chemistry*, 2015, **87**, 10585-10592.
60. J. Kim, H. Cho, S.-I. Han and K.-H. Han, *Analytical Chemistry*, 2016, **88**, 4857-4863.
61. H. Wang, N. Sobahi and A. Han, *Lab on a Chip*, 2017, **17**, 1264-1269.